

# Toward Explainable Heat Load Patterns Prediction for District Heating

## Authors

L. Minh Dang<sup>1</sup>, Jihye Shin<sup>2</sup>, Yanfen Li<sup>3</sup>, Lilia Tightiz<sup>4</sup>, Tan N. Nguyen<sup>5</sup>, Hyoung-Kyu Song<sup>1</sup>, and Hyeonjoon Moon<sup>3,\*</sup>

## Affiliations

1. Department of Information and Communication Engineering and Convergence Engineering for Intelligent Drone, Sejong University, Seoul, South Korea

2. Department of Artificial Intelligence, Sejong University, Seoul, South Korea

3. Department of Computer Science and Engineering, Sejong University, Seoul, South Korea

4. School of Computing, Gachon University, 1342 Seongnam-daero, Sujeong-gu, Seongnam-si, 13120, Gyeonggi-do, Republic of Korea

5. Department of Architectural Engineering, Sejong University, 209 Neungdong-ro, Gwangjin-gu, 05006, Seoul, Republic of Korea

corresponding author(s): Hyeonjoon Moon (hmoon@sejong.ac.kr)

## Abstract

Heat networks play a vital role in the energy sector by offering thermal energy to residents in certain countries. Effective management and optimization of heat networks require a deep understanding of users' heat usage patterns. Irregular patterns, such as peak usage periods, can exceed the design capacities of the system. However, previous work has mostly neglected the analysis of heat usage profiles or performed on a small scale. To close the gap, this study proposes a data-driven approach to analyze and predict heat load in a district heating network. The study uses data from over eight heating seasons of a cogeneration DH plant in Cheongju, Korea, to build analysis and forecast models using supervised machine learning (ML) algorithms, including support vector regression (SVR), boosting algorithms, and multilayer perceptron (MLP). The models take weather data, holiday information, and historical hourly heat load as input variables. The performance of these algorithms is compared using different training sample sizes of the dataset. The results show that boosting algorithms, particularly XGBoost, are more suitable ML algorithms with lower prediction errors than SVR and MLP. Finally, different explainable artificial intelligence approaches are applied to provide an in-depth interpretation of the trained model and the importance of input variables.

## Introduction

District heating (DH) has risen as a crucial energy supply infrastructure in order to effectively provide heat and cooling to consumers over the last few decades<sup>1</sup>. DH is superior in many aspects compared to other energy supply options, which include having a lower carbon footprint, the integration of multiple heat sources, and high energy throughput. The latest fourth and fifth generations of DH can utilize several heat sources, which include combined heat and power (CHP), gas boilers, water-source heat pumps (HPs), ground-source HPs, and solar energy-based HPs. The recent literature focused more on developing simulation frameworks and effective approaches in regards to designing and optimizing DH systems in terms of the economic and energetic factors, which is due to the fast development of DH technologies<sup>2,3</sup>. Storage technology is also a hot topic, because it helps decouple heat production and the demand to increase DH efficiency<sup>4</sup>. The following articles<sup>1,5</sup> were reviewed in order to obtain the latest information about DH networks.

51 The heat usage pattern analysis has become increasingly essential as the number of end-users  
52 increases, because it greatly impacts the entire network's efficiency. Variations in the heat  
53 usage behavior from the consumers' side lead to variations in the heat usage pattern of a  
54 single substation, which is a major matter for accurate and efficient DH management and  
55 operation<sup>6</sup>. For example, the substantial temperature difference between the summer and  
56 the winter significantly influences the users' heat demand. In addition, the hourly heat  
57 demand also varies between households, which causes heat demand variation at the  
58 substation<sup>7</sup>.

59  
60 An accurate heat demand prediction framework is imperative in order to effectively manage  
61 DH networks<sup>8</sup>. First, it facilitates the optimization of the overall heat production, minimizes  
62 the heat loss, and optimizes the operating costs. Second, the distribution temperature is  
63 provided at an appropriate range in order to predict the real-time heat usage using the heat  
64 demand forecast model. As a result, the number of studies proposed in regards to predicting  
65 the heat demand has been increasing. A heat demand analysis can generally be divided into  
66 model-based and data correlation categories<sup>9</sup>. The data correlation approach mainly depends  
67 on building functional correlations of the DH parameters in order to develop a heat usage  
68 profile for each substation or building. The model-based technique relies on machine learning  
69 (ML) algorithms in order to effectively learn the representative patterns using the historical  
70 heat load data<sup>10</sup>. The data correlation approach offers higher accuracy than the model-based  
71 approach, but it is time-consuming and laborious due to each building/substation having a  
72 unique heat usage profile that needs to be constructed. The performance of the model-based  
73 heat usage prediction algorithm has become significantly better, which is due to the huge  
74 advancements in artificial intelligence (AI) and big data over the past few decades<sup>9,10</sup>.

75  
76 The heat usage prediction, heat loss estimation, and abnormality analysis based on the energy  
77 signature (ES) have been increasingly investigated in recent years, which have shown  
78 promising results<sup>11,12</sup>. However, these studies mainly used outdoor temperature as the main  
79 feature in order to discover the heat demand pattern. Other studies focused on peak usage  
80 forecasting with the ultimate objective of optimizing the energy usage and DH management<sup>13</sup>.  
81 These studies, which are similar to the ES, failed to consider the meteorological data or the  
82 end-user behaviors. Potential influencers of the heat demand patterns can be divided into  
83 three main factors, which include meteorology, behaviors, and time<sup>14</sup>. Some common  
84 meteorological data that potentially affects heat demand are humidity, solar irradiation,  
85 outdoor temperatures, and the wind flow speed<sup>15</sup>. Time factor involves all time-related  
86 parameters, which include hours, days, months, and years. The social behaviors of the end-  
87 users are also a crucial influencer of the heat load variation, which can be affected by both  
88 meteorological and time factors<sup>16</sup>. These three main factors significantly influence the heat  
89 demand patterns.

90  
91 There has been considerable interest in the research area of heat load forecasting for DH, as  
92 indicated by numerous recent studies. Idowu et al.<sup>29</sup> examined a range of supervised ML  
93 algorithms in order to perform heat load prediction up to 48 hours in advance. The  
94 experimental results revealed that conventional ML algorithms, such as SVM and linear  
95 regression, achieved the lowest normalized root mean square error when compared to other  
96 algorithms. In another study, Boudreau et al. found that ensemble models provided  
97 significantly better prediction accuracy than base ML models when it came to predicting peak  
98 power demand and next-day building energy usage<sup>30</sup>.

99  
100 Several studies have delved into specific aspects of DH systems. For example, Saloux et al.  
101 explored the application of ML algorithms for predicting the aggregated heating usage of a  
102 community. They concluded that the models' performance could be significantly enhanced by

103 considering other crucial factors, such as time of day, systematic variables, and temperature<sup>31</sup>.  
104 López et al. focused on the impact of specific days, such as holidays or festive periods, on the  
105 load curve, and determined that such events could considerably affect the heat usage  
106 pattern<sup>32</sup>. Moreover, a case study of a large DH network over several heating seasons revealed  
107 that the primary force of heat demand were the various operation settings during daytime  
108 (night shutdown and night temperature setback) and the outdoor temperature<sup>33</sup>.

109  
110 Despite the numerous issues addressed and methods discussed in existing literature on heat  
111 load prediction in DH networks, further research is needed to explore important external  
112 factors such as holiday and weather conditions, which could be utilized as input to improve  
113 the models' accuracy<sup>6</sup>. Additionally, while previous work has showed the high predictive  
114 performance of ML algorithms for heat demand, they have not provided a clear explanation  
115 of why the model achieved good performance, as well as which features are important and  
116 their correlation with the models<sup>10</sup>.

117  
118 This research is proposed in order to improve the heat usage prediction via an in-depth  
119 analysis of the dataset to figure out the potential factors that impact the heat demand. The  
120 main contributions include (a) performing a data analysis prior to the training process to help  
121 thoroughly understand the dataset, (b) training and comparing different ML models in order  
122 to obtain the best hourly heat load prediction model, and (c) offering detailed explanations  
123 about what features were imperative to the model prediction, which were overlooked in the  
124 previous studies.

125  
126 The remainder of the manuscript is outlined as follows. Section "Dataset description" gives a  
127 detailed description of the proposed heat demand dataset. After that, the Section  
128 "Methodology" outlines all processes involved in heat demand prediction. Several  
129 experiments are performed in Section "Experimental results" to comprehensively assess the  
130 proposed framework. Next, the Section "Discussion" discusses the findings and provides a  
131 detailed analysis of the study. Finally, we conclude the study and offer future work in the  
132 Section "Conclusion".

133

## 134 **Dataset description**

135 The dataset that is described in this research was the hourly heat demand from an eco-friendly  
136 liquefied natural gas (LNG)-based cogeneration plant in the Cheongju region, Korea. The plant  
137 produces around 76.5 Gigacalories (Gcal) of local heating to the distribution grid. Gcal is a  
138 common heat load unit, which measures the heat energy in the heating plants. The LNG-  
139 powered plant is more efficient and environmentally friendly for the generation of thermal  
140 energy, which has been reported to produce over 70% less emission than coal or oil sources.

141

142 The dataset introduced in this study includes the hourly heat usage from January 2012 to  
143 December 2020 of the residents from a region, which spans eight heating seasons from  
144 November to April. The heat usage profile suggests the amount of heat that is transmitted  
145 from the plant to the consumers at a specific duration, which mainly involves space heating  
146 (SH) and domestic hot water (DHW). The corresponding hourly historical weather data was  
147 also collected as an additional feature in order to discover the potential connections with the  
148 heat load patterns in addition to the heat load data. A holiday feature that indicates whether  
149 the day under consideration is a holiday is also added in order to investigate the end-user  
150 behaviors. The three main features that belong to the weather data include wind flow speed,  
151 humidity, and outdoor temperature. The collected heat usage dataset is used to study the  
152 hourly heat load patterns and provides some explanations for the model's predictions. The  
153 minimum, maximum, mean and standard deviation for each variable are described in Table 1.

154

155  
156

**Table 1:** Description of important observations with possible values for the variables in the proposed dataset

Name	Minimum   Maximum	Mean   standard deviation	Unit
Date	01/01/2012   01/01/2022	-	-
Wind speed	0   8.7	1.47   0.93	m/s
Humidity	7   100	61.32   20.02	%
Outdoor temperature	-16.5   38.1	13.75   10.83	°C
Holiday	0 (normal day)   1 (holiday)	0.32   0.46	-
Heat load	0   317	65.89   52.92	Gcal

157  
158  
159  
160  
161  
162  
163  
164

In summary, 8760 hourly heat load profiles and their corresponding historical temperature data are obtained yearly. Therefore, a total of 87,672 entries, which include date and time, holiday, wind flow speed, humidity, and temperature, are used as the input variables, and the heat load profiles are used as the target variables. The data entries from 2012 to 2020 were used as the training set, whereas the hourly heat usage of 2021 was applied in order to test the model's performance.

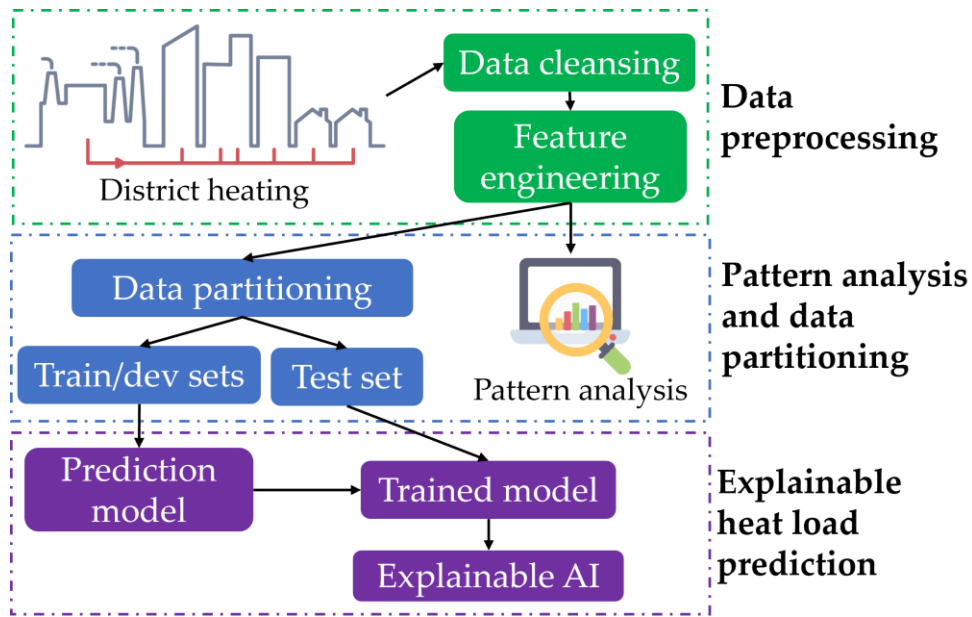
165  
166  
167  
168

## Methodology

Figure 1 depicts the three components of the hourly heat usage prediction system, which are (a) data preprocessing, (b) pattern analysis and data partitioning, and (c) explainable heat load forecasting.

169  
170  
171  
172  
173  
174  
175  
176  
177  
178  
179  
180  
181  
182

- Data preprocessing: There is a high possibility that the structured data may contain some common issues with data preprocessing, such as duplicate data, missing data, and negative data due to human errors, which can affect the system's performance. As a result, it is a prerequisite before the data analysis and training processes to fix all errors and standardize the data.
- Pattern analysis and data partitioning: Heat usage patterns play an important role in regards to enabling specialists to study consumer behavior. The distinctive patterns of the dataset are discovered in this section by using various data analysis approaches in order to thoroughly analyze the dataset before the training phase. The dataset is then divided into training and testing sets.
- Explainable heat load prediction: Different ML algorithms were trained in order to forecast the hourly heat usage. Some explainable artificial intelligence (XAI) approaches are finally implemented in order to interpret the model's predictions.



183  
184 **Figure 1:** Description of the primary components of the heat usage patterns analysis  
185 framework

186  
187 **Data Preprocessing**

188 **Data cleaning**

189 The structured data-related issues, such as missing and duplicated data are unavoidable during  
190 the data collection, and they can negatively affect the model's performance if not  
191 appropriately corrected. Data cleansing is therefore conducted in order to detect and fix error  
192 records in regards to the humidity, wind speed, outdoor temperature, and hourly heat usage  
193 data. There are various data cleaning processes, and the two main processes that were  
194 performed in this study include removing duplications and fixing the missing values. The  
195 dataset is loaded as a data frame using pandas, a famous data manipulation and analysis  
196 library. After that, data inconsistencies can be automatically detected using pandas-supported  
197 functions.

198  
199 Standard techniques, such as moving average (MA) and imputation, are usually employed in  
200 order to correct the missing data. This study applied the exponential weighted moving average  
201 (EWMA) technique<sup>17</sup>, which is an extension of the MA algorithm. EWMA considers the recent  
202 data points to be significantly important with a higher weight, whereas the data points in the  
203 further past receive an exponentially lower weight. Moreover, the EWMA method can be  
204 effectively applied due to the nature of the dataset, and the differences between the two  
205 consecutive data points are considered minor. The EWMA can be described as follows.

206  
207 
$$E_t = \alpha \times x_t + (1 - \alpha) \times E_{t-1} \quad (1)$$

208  
209 where  $E_t$  indicate the computed value at time t based on the EWMA technique.  $x_t$  is the value  
210 of the series in the current period.  $E_{t-1}$  is the EWMA at the previous time period. Finally,  $\alpha$  is  
211 the smoothing factor, which ranges between 0 and 1 and controls the influence of the current  
212 value  $x_t$  on the  $E_t$ . A larger  $\alpha$  places more weight on recent observations and results in a more  
213 reactive EWMA, while a smaller  $\alpha$  results in a smoother EWMA.

214  
215 **Feature engineering**

216 Feature engineering is the process of selecting, extracting, and transforming relevant features  
217 or variables from raw data to enhance the performance of ML algorithms. The goal of feature  
218 engineering is to provide ML algorithms with informative and discriminative features that can  
219 help them better understand the underlying patterns and relationships in the data. Two main  
220 processes in the feature engineering process are standardization and feature transformation.  
221

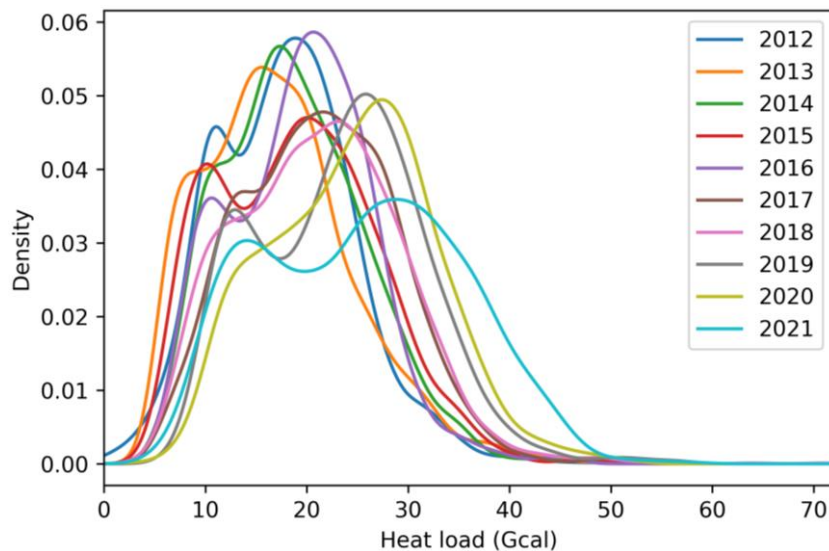
222 The regression model fitting and learned function can be negatively affected by structured  
223 data, and it eventually creates a bias when numerical features with different scales are fed  
224 into the model<sup>18</sup>. The normalization/standardization techniques therefore need to be  
225 implemented in order to normalize the input features. Min-max normalization and  
226 standardization are two common feature scaling approaches<sup>19</sup>. The heat usage dataset that is  
227 applied to fit the model contains peak heat load on some specific periods, which are outliers,  
228 and it has an essential role during the training process. The min-max normalization likely  
229 lowers the impact of those outliers by transforming all features into a range between 0 and  
230 1. The standardization therefore scales the features in order to have a zero mean, and a  
231 standard deviation of 1 is implemented in this study.  
232

233 Feature transformation is necessary for structured data in order to convert categorical inputs  
234 into numerical inputs, because most ML models work with numerical data. The holiday  
235 variable is categorical, because it has two distinctive values, which represent whether a  
236 particular day is a regular day or a holiday. As a result, one-hot encoding, which creates a  
237 binary representation of the categorical feature, is applied in order to transform the holiday  
238 feature<sup>20</sup>. For instance, when a specific day is a holiday, the value for the holiday binary  
239 variable is set to 1, and the regular binary variable is 0.  
240

## 241 **Pattern Analysis and Data Partitioning**

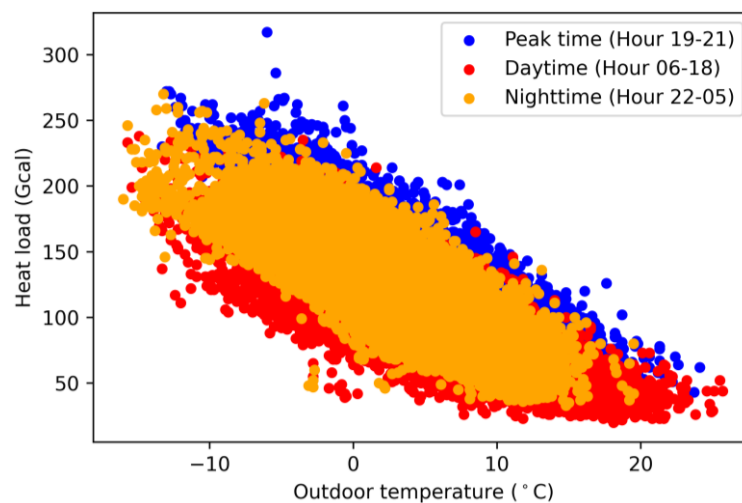
### 242 ***Pattern analysis***

243 **Heat network during the summer season:** The investigation of the heat network in the  
244 summer season, which spans from June to August, gives some exciting insights into the town's  
245 heat usage. Figure 2 illustrates the hourly heat demand distribution density for the summer  
246 months from 2012 to 2021. The average heat demand in the summer mainly involves the DHW  
247 consumption and the network heat losses. It can generally be seen that there was less heat  
248 demand in the distant past compared to the recent years. For instance, a roughly similar  
249 distribution can be observed for the following years, which include from 2012 to 2016, with  
250 the average heat demand being around 20 Gcal. However, the average heat demand increased  
251 to around 30 Gcal, which included the more recent years from 2019 to 2021, with some higher  
252 heat demands being related to particular heat usage patterns. Moreover, there has been a  
253 gradually increasing trend in the average heat usage of over 40 Gcal in recent years, and the  
254 year 2021 shows the highest density.



255  
256 **Figure 2:** Distribution density plot of hourly heat demand during the summer season  
257 (Jun.-Aug.)

258  
259 **Heat network during the winter season:** The chart in Figure 3 illustrates the network's energy  
260 consumption on an hourly basis during the winter season spanning from November to March.  
261 The chart depicts three distinct patterns for three different time periods: daytime (06:00 to  
262 18:00), nighttime (22:00 to 05:00), and peak hours (19:00 to 21:00). The scatter plot reveals  
263 that the consumers tend to use more heat during the peak time at the same temperature level  
264 compared to the nighttime and daytime. Moreover, the lower the outside temperature, the  
265 higher the heat load that is required.



266  
267 **Figure 3:** Scatter plot of the outdoor temperature and the heat usage during the winter  
268 season (Nov.-Mar.)

269  
270 **Some heat load patterns for each season of the year:** A typical hourly heat load pattern for  
271 each season can be observed in Figure 4. The spring, fall, and winter seasons have similar  
272 variations in the hourly time scale, which is caused by the social behavior of the end-users.  
273 Reduced heat loads can be observed in the daytime, which is due to solar radiation that leads  
274 to higher daytime temperatures. The highest heat load during the daytime occurs around 8  
275 am in order to prepare the space heating in offices and commercial buildings. The heat  
276 demand usually peaks between 19:00 and 21:00 because of the low temperature at night,  
277 which requires more heat for SH and DHW. DHW is a major part of the heat demand in the  
278 summer, when a tiny difference in the heat variation can be observed.

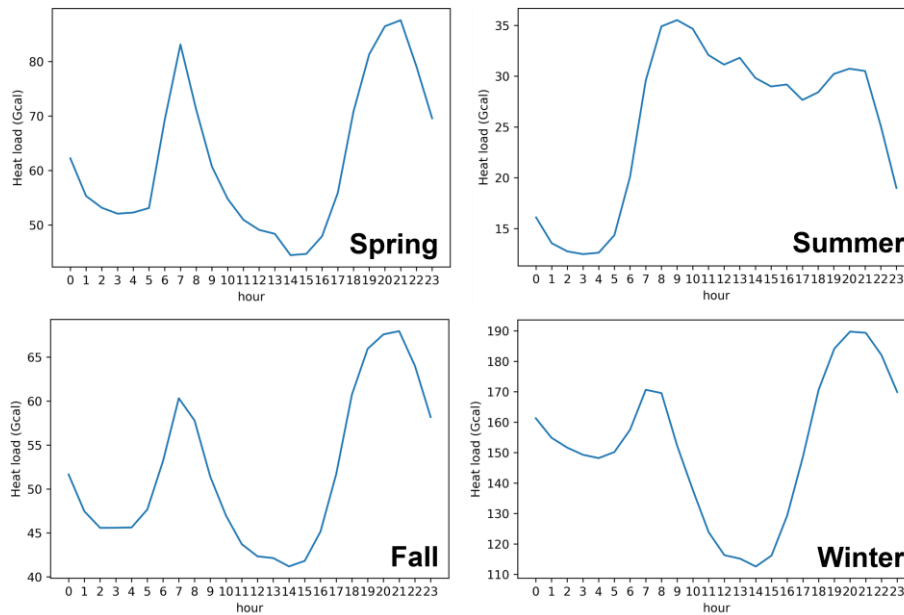


Figure 4: Average weekly heat load patterns during the four season periods

279

280

281

282

### Data partitioning

283

Data partitioning is a fundamental step required before training and evaluating the model. After preprocessing, the data is split into two sets: the training set and the testing set. The training set is utilized to train and optimize the model, while the testing set is typically employed to assess the algorithms' performance across various scenarios. This study used the heat usage profiles between 2012 and 2020 as the training set, whereas the heat load profiles from 2021 were used for the testing. Each training or testing sample consists of day, hour, outdoor temperature, humidity, windspeed, and holiday as the input variables, while the output is the hourly heat usage corresponding to that particular input.

289

290

291

292

### Explainable Heat Load Prediction

293

This section presents the main concepts behind boosting, support vector regression (SVR)<sup>21</sup>, and multilayer perceptron (MLP) algorithms<sup>22</sup> that were implemented for the heat demand forecasting.

294

295

296

297

**Boosting algorithms:** Boosting algorithm belongs to the ensemble approach, which sequentially adds multiple weak learners. Each weak learner is added by using the learned information from its predecessor, and it tries to correct the errors that are predicted by them. A weak learner can be any learning algorithm that offers a slightly better performance than random guessing. Two standard boosting approaches are gradient boosting and adaptive boosting<sup>23</sup>.

298

299

300

301

302

303

- Adaptive boosting: The adaptive boosting (AdaBoost) algorithm was proposed by sequentially adding weak learners, which involved using decision trees, and attempting in order to correct the wrongly predicted samples by applying a bigger weight to them during the training process of the latter weak learners. The AdaBoost model's final output is the weighted median.

304

305

306

307

308

- Gradient boosting: AdaBoost assigns new instance weights whenever a new weak learner is added, but gradient boosting aims to fit the new predictor to the residual errors that are caused by the prior predictor with the primary objective of minimizing a loss function<sup>24</sup>. Some popular gradient boosting algorithms include LightGBM and XGBoost.

309

310

311

312



313 XGBoost leverages the feature distribution across all data points to narrow down the search  
314 space of potential feature splits. The objective of the XGBoost algorithm can be expressed as:

$$315 \quad \text{objective} = L + \mu \quad (2)$$

317 where the predictive ability of XGBoost is determined by the loss function  $L$ , while the  
318 regularization term  $\mu$  is used to manage overfitting.  $\mu$  is determined by the number of  
319 observers and their prediction threshold in the ensemble model. Since the problem in  
320 question belongs to regression analysis, the root mean squared error (RMSE) is used as the  
321 loss function  $L$ .

322  
323  
324 **Support vector regression (SVR):** Unlike typical regression algorithms that seek to minimize  
325 the sum of squared errors between actual and predicted values, SVR attempts to identify the  
326 optimal hyperplane within a user-defined threshold value. The threshold value is the distance  
327 between the boundary line and the hyperplane. Heat demand prediction is a complex non-  
328 linear topic, because it has multiple input variables. To address non-linearity in the initial  
329 feature space and treat it as a linear problem in the high-dimensional feature space, SVR  
330 requires the use of a non-linear kernel. The Gaussian Radial Basis kernel (RBF) was used in this  
331 study as the default kernel for SVR.

332  
333 **Multilayer perceptron (MLP):** Multilayer perceptron (MLP) belongs to the feedforward  
334 artificial neural networks (ANN) category. MLP's fundamental structure consists of an input  
335 layer, one or more hidden layers with neurons, and an output layer that are stacked in  
336 sequence. The neuron is the primary computing component of MLP, and neurons from the  
337 current layers fully connect to neurons from the next layer. The inputs are added to the initial  
338 weights, fed into an activation function, and propagated to the next layer.

339

## 340 **Experimental results**

341 This section shows all experiments that were conducted to determine the most suitable  
342 algorithm for predicting heat usage. In addition, various XAI techniques were also conducted  
343 in order to provide an in-depth analysis of the trained models.

344  
345 The heat load prediction models were constructed and trained on scikit-learn<sup>28</sup>, a Python-  
346 based open-source ML library. Three main explainable AI libraries for analyzing the data  
347 include partial dependence plot<sup>27</sup> (PDP), which is a global and model-agnostic XAI algorithm,  
348 local interpretable model-agnostic explanations<sup>39</sup> (LIME), which create a local model  
349 approximation of the model around the prediction of interest, and shapley additive  
350 explanations<sup>26</sup> (SHAP), which employ a game-theoretic approach.

351

## 352 **Evaluation Metrics**

353 Three standard evaluation metrics were computed, which included the coefficient of  
354 determination ( $R^2$ ), mean squared error (MSE), and mean absolute error (MAE) in order to  
355 evaluate the heat demand forecasting. MSE is computed by averaging the squared difference  
356 between the predicted values and actual values for all the training samples<sup>25</sup>. On the other  
357 hand, MAE is the average of the absolute differences between the predicted values and true  
358 values. While MSE measures the standard deviation of residuals, MAE calculates the average  
359 of the residuals in the dataset.  $R^2$  is computed by determining the proportion of the  
360 dependent variable's variance predicted by the algorithm. The lower the MSE and MAE scores,  
361 the better the model's performance. However, a higher value of  $R^2$  is considered better. The  
362 three metrics can be formulated as follows.

363

364 
$$MSE = \frac{1}{N} \sum_{i=1}^N (y_i - \hat{y}_i)^2 \quad (3)$$

365 
$$R^2 = 1 - \frac{\sum (y_i - \hat{y}_i)^2}{\sum (y_i - \bar{y})^2} \quad (4)$$

366 
$$MAE = \frac{1}{N} \sum_{i=1}^N |y_i - \hat{y}_i| \quad (5)$$

367

368 where  $N$  is the total number of training samples.  $y_i$  indicates the actual value,  $\hat{y}_i$  means the  
 369 predicted value of the  $i$ th profile, and  $\bar{y}$  is the mean value of  $y$ .

370

371 **Hyperparameter Fine-tuning**

372 Five regression models were implemented in this study in order to perform the heat demand  
 373 forecasting, which included SVR, AdaBoost, XGBoost, LightGBM, and MLP. Each model has its  
 374 crucial hyperparameters that must be determined before the training. The hyperparameters  
 375 control the training behavior of the learning algorithms, and they considerably influence the  
 376 model's performance.

377

378 Table 2 shows the hyperparameters and the value range for each hyperparameter that is  
 379 required by the five models. A grid search method was conducted next on the different  
 380 combinations of the hyperparameters of each algorithm in order to explore the most suitable  
 381 hyperparameter combination that helps the algorithm obtain the best performance.

382

383 **Table 2:** Initial hyperparameter value ranges and the optimal hyperparameter value for each  
 384 algorithm

Model	Hyper parameter	Definition	Value ranges	Optimal value
AdaBoost	$n$	Number of estimators	50, 100, 150, 200	50
	$\sigma$	Learning rate	$10^{-3}, 10^{-2}, 10^{-1}$	$10^{-1}$
XGBoost	$n$	Number of estimators	50, 100, 150, 200	50
	$d_{tree}$	Max depth of a tree	3, 6, 9, 12, 15	9
	$\gamma$	Min loss reduction	0, 0.1, 0.2, 0.3	0
	subsample	Subsample ratio of the training instances	0.5, 1, 2	1
LightGBM	num_leaves	Max number of nodes per tree	21, 31, 41, 51	31
	$\sigma$	Learning rate	$10^{-3}, 10^{-2}, 10^{-1}$	$10^{-1}$
	$n$	Number of estimators	50, 100, 150, 200	100
SVR	$d_{tree}$	Max depth of a tree	2, 3, 4, 5, 6	4
	$C$	Regularization parameter	$10^0, 10^1, 10^2, 10^3$	$10^0$
	$\gamma$	Kernel coefficient	$10^{-6}, 10^{-3}, 10^{-1}$	$10^{-3}$
MLP	$\sigma$	Learning rate	$10^{-3}, 10^{-2}, 10^{-1}$	$10^{-2}$
	$nh_i$	Number of neurons in hidden layer $i^{th}$	50, 100, 150, 200	150
	$\varphi$	Activation function	ReLU, tanh	ReLU
	B	Batch size	8, 16, 32, 64	32

385

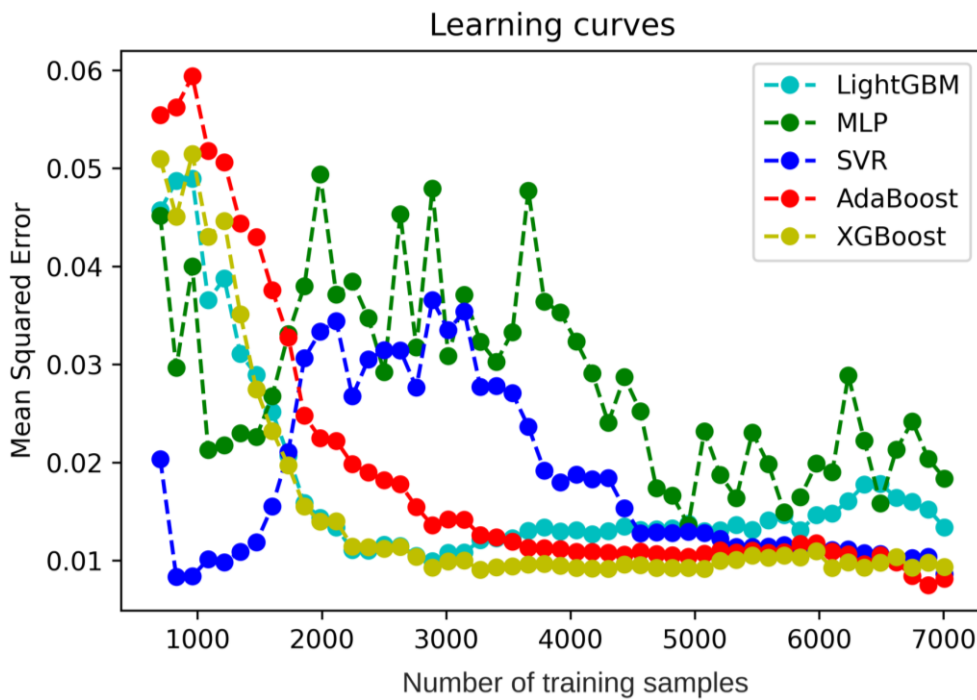
386

387 **Heat Usage Prediction Analysis**

388 Figure 5 depicts the performance and scalability comparison of five different learning  
 389 algorithms using the learning curves in order to show the effect of adding more samples during

390 the training process. The experiment involved randomly selecting samples from the training  
 391 dataset. A training sample include date, outdoor temperature, windspeed, humidity, holiday,  
 392 and hourly heat demand as the features.

393  
 394 It can generally be concluded that SVR and MLP were highly sensitive to the dataset size,  
 395 because they widely fluctuated as more training samples were added. On the other hand, the  
 396 boosting algorithms, which included AdaBoost, LightGBM, and XGBoost, showed their  
 397 advantages and effectiveness with a bigger dataset. The three ensemble algorithms exhibited  
 398 similar trends in variation; the error gradually decreased and eventually stabilized. Low MSE  
 399 scores of less than 0.02 were obtained for the three boosting algorithms when the training  
 400 dataset size was over 2000 samples. XGBoost achieved the lowest mean squared error of less  
 401 than 0.01 among the three algorithms, and it showed its robustness when the number of  
 402 training samples reached 7000. As a result, XGBoost was utilized as the primary model for the  
 403 following experiments.



404  
 405 **Figure 5:** Heat demand forecasting performance using five different algorithms

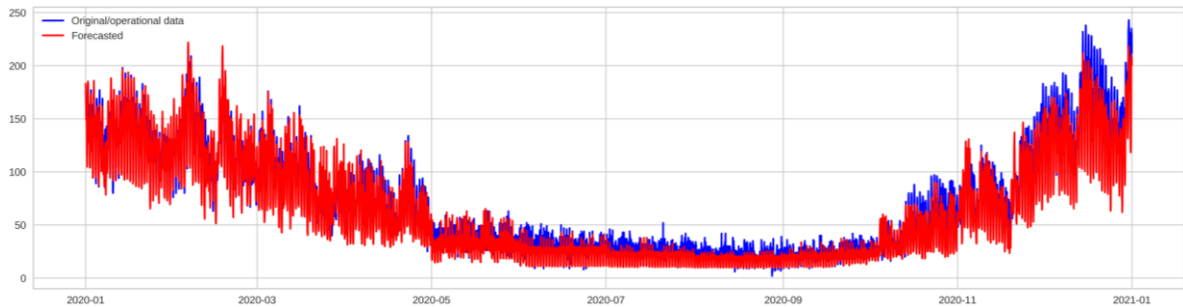
406  
 407 Table 3 shows the heat demand forecasting performance using five ML algorithms on the test  
 408 dataset. All the models generally obtained good performances on the dataset. The boosting  
 409 algorithms performed better than SVR and MLP. The XGBoost algorithm achieved the highest  
 410  $R^2$ , MSE, and MAE at 0.95, 0.12, and 0.15, respectively. On the other hand, MLP showed the  
 411 lowest heat usage prediction performance with an MSE value of 0.25 and  $R^2$  at 0.89.

412  
 413 **Table 3:** Hourly heat load prediction performance for the five ML algorithms on the testing  
 414 dataset.

Model	MAE	MSE	$R^2$
AdaBoost	0.16	0.14	0.94
XGBoost	0.15	0.12	0.95
LightGBM	0.18	0.17	0.91
SVR	0.24	0.21	0.92
MLP	0.23	0.25	0.89

415

416 Figure 6 compares the actual and the predicted heat demand for 2021 using the XGBoost  
417 model. The heat usage values predicted by the model, which are illustrated by the red line,  
418 are roughly similar to the actual heat usage values, which are illustrated by the blue line.  
419 Moreover, each month's peak and bottom heat usage were accurately predicted. However,  
420 the model performance was significantly affected, which is due to some uncommon end-user's  
421 heat usage behaviors.



422

423 **Figure 6:** Daily heat load prediction results on the testing dataset

424

### 425 **Explainable Heat Usage Prediction**

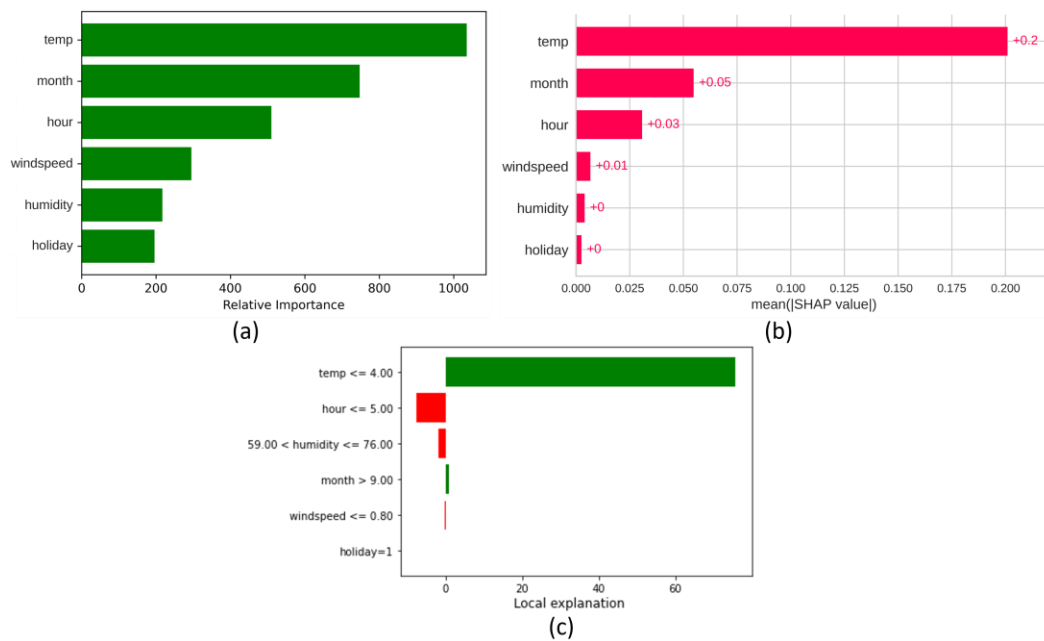
426 The previous section discussed what model achieved the highest heat usage forecasting  
427 performance. However, it is challenging to reveal what features are influential and how they  
428 affect the model predictions. As a result, some interesting XAI approaches are implemented  
429 in this section in order to attempt to explain how ML models predict the outcomes.

430

431 Firstly, three different feature ranking techniques were implemented in order to evaluate each  
432 feature's importance in regards to predicting the output heat usage by the model, as displayed  
433 in Figure 7. Figure 7(a) calculates a feature's relative importance by examining the mean and  
434 standard deviation of impurity reduction across each tree. Figure 7(b) ranks the feature  
435 importance by computing the game's theoretically optimal shapley values<sup>26</sup>. The resulting  
436 shapley values provide a measure of the relative importance of each feature in the model  
437 prediction for a particular data point. It requires examining every possible feature combination  
438 and assessing the marginal impact of each feature on the prediction. Features with higher  
439 Shapley values are regarded as more significant. Ranking both approaches reveal that the  
440 temperature and month features are crucial, which is valid due to the end-users heat demand  
441 pattern being significantly affected by these two features.

442

443 Finally, Figure 7(c) visualizes the feature importance assessed by LIME. Positive weights  
444 indicate that a feature promotes a positive prediction, while negative weights indicate the  
445 opposite. The magnitude of the weight represents the importance of the feature. It is  
446 noticeable that a temperature of 4°C or lower (cold season) presses the model to output a  
447 higher heat usage.



448

449 **Figure 7:** Feature importance analysis for the heat usage prediction model

450

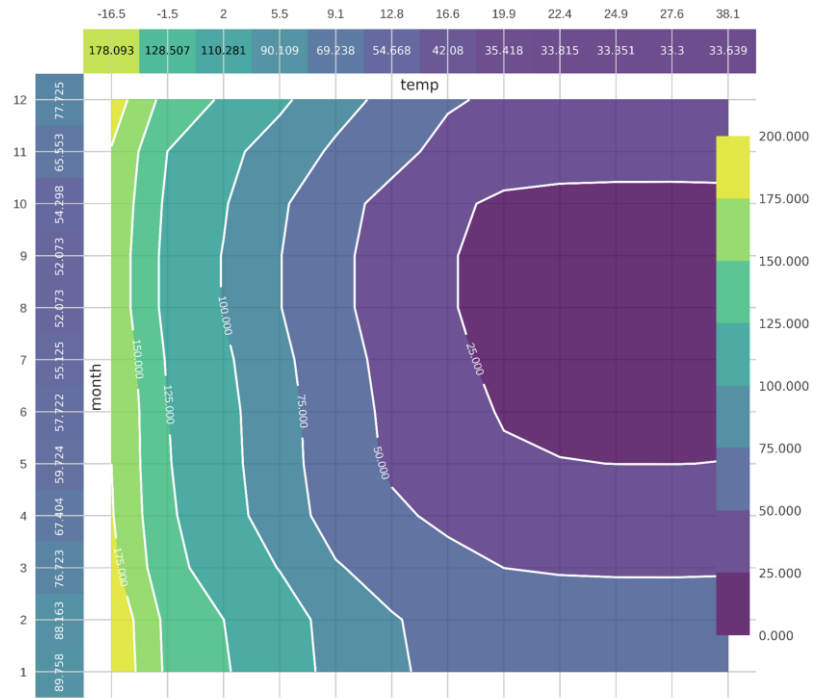
451 The previous experiment indicated that the temperature and month features greatly impacted  
 452 the model's predictions, but it did not explain exactly how the model was affected. As a result,  
 453 PDP, was implemented in order to demonstrate a feature's marginal effect on the models'  
 454 prediction.

455

456 Figure 8 shows how temperature and month together impact heat usage in the form of  
 457 contour lines. Contour was proved to work best for analyzing the impact of continuous  
 458 features in the PDP interaction plot<sup>38</sup>.

459

460 The contour lines, ranging from 0.000 to 150.000, indicate how specific ranges of the two  
 461 features affect heat usage. A higher value of the contour line implies a greater impact of the  
 462 two features on heat usage. For example, during the summer season when the average  
 463 temperature is above 22°C, the features have a negative influence on the model prediction,  
 464 resulting in an average heat demand of less than 50 Gcal and a contour line value of under  
 465 25.000. On the other hand, contour line values greater than 125.000, corresponding to the  
 466 winter season with an average temperature of fewer than 2°C, positively impact the model  
 467 prediction leading to the average heat usage of over 120 Gcal.



468

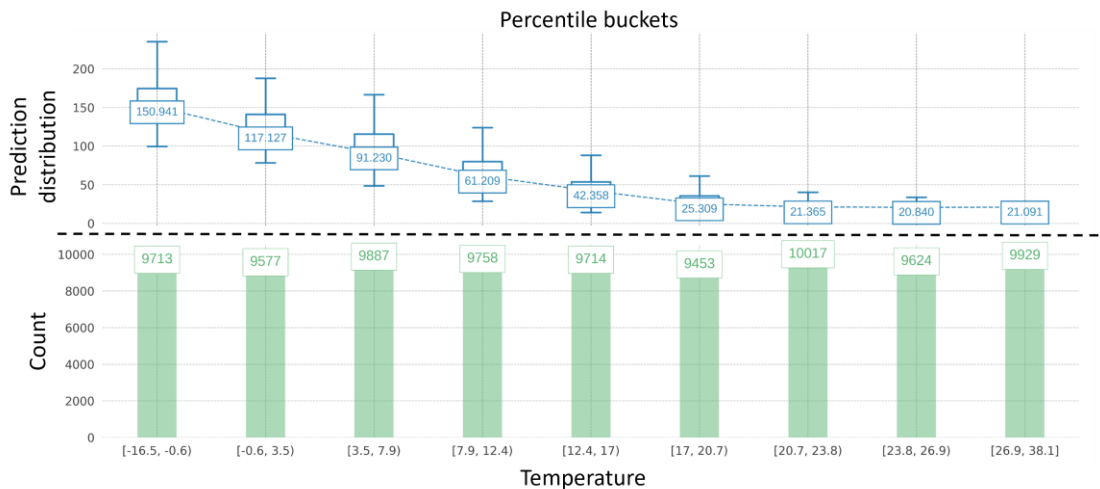
469 **Figure 8:** PDP interaction plot for the temperature and month features

470

471 Figure 9 illustrates how the temperature feature affected the heat demand through the  
 472 distribution of the actual heat demand via fixed values of the temperature variable. It was  
 473 observable that the hourly heat load achieved the biggest average value, which was  
 474 approximately 150 Gcal, occurred when the temperature feature was between  $-16.5^{\circ}\text{C}$  to  $-0.6^{\circ}\text{C}$ ,  
 475 indicating the winter season. Moreover, the hourly heat demand gradually dropped when  
 476 the temperature rose. The lowest hourly heat demand, around 21 Gcal, was recorded when  
 477 the temperature ranged from  $26.9^{\circ}\text{C}$  to  $38.1^{\circ}\text{C}$ , which corresponds to the summer season.

478

479 Based on the data, we can conclude that the hourly heat demand is directly proportional to  
 480 the temperature. In the summer, DHW accounts for the majority of the heat demand. In  
 481 contrast, both DHW and SH contribute to the heat demand during the winter. Additionally,  
 482 the hourly heat demand is higher during the winter, with temperatures below  $10^{\circ}\text{C}$ , and lower  
 483 during the summer, with temperatures above  $26^{\circ}\text{C}$ .



484

485 **Figure 9:** Actual predictions plot for the temperature variable. Distribution of the actual

486 prediction via different variable values

487

## 488 **Comparison with Similar Studies**

489 Numerous studies have been conducted in the past to predict and analyze DH head demand.  
490 However, direct comparisons with these studies are difficult due to differences in DH network  
491 designs, input data, and architecture implementations or experimental setups. We use  
492 operational data from DHS to predict heat usage patterns and compare our results using the  
493 XGBoost model, which exhibits the best prediction performance. The recorded MAE value  
494 from this study was 15%, which is smaller than the reported MAE of 18.07% by Huang et al<sup>34</sup>.  
495 In addition, the computed evaluation metrics are also superior to the following research<sup>35,36</sup>.  
496 Specifically, the proposed XGBoost model outperforms the study suggested by Ivanko et al<sup>36</sup>  
497 in terms of MSE and correlation coefficient, achieving 12% and 0.95 on the testing set,  
498 respectively, compared to MSE of 45.04% and a coefficient of determination of 0.81. In terms  
499 of the correlation coefficient, the XGBoost method also shows better hourly prediction  
500 performance than the ANN model proposed by Bünning et al<sup>35</sup>, with a correlation coefficient  
501 of 0.95 for one hour compared to 0.88.

## 502 **Discussion**

503 This section provides a discussion based on our approach and the obtained results.  
504 Furthermore, a discussion about the interpretability of the study is also presented.

505

## 506 **Model Performance**

507 To establish the best heat demand prediction model, five different models were evaluated  
508 with varying sizes of training datasets. Then, three evaluation metrics (MSE, MAE, and  
509  $R^2$ ) were calculated. Figure 5 demonstrates the learning trend of these models as the number  
510 of training samples increases. When the training dataset size is less than 2000, MLP and SVR  
511 exhibit the highest accuracy. However, these models have drawbacks such as the need for  
512 sequential data and extended training times, making them more suitable for applications that  
513 can handle longer training periods. On the other hand, for larger training datasets (over 2000  
514 samples), the accuracy of the three boosting algorithms is higher. Boosting algorithms, such  
515 as AdaBoost and XGBoost, are more appropriate for granular control and frequent updating  
516 due to their short training time, stability, and forecasting accuracy. Nonetheless, all models  
517 can generate predictions swiftly (within a second) after being trained. Hence, the time  
518 required for training and retraining the models is the primary constraint for their overall  
519 implementation.

520

521 Collinearity, which refers to the correlation between predictor variables, always exists in real-  
522 world data<sup>24</sup>. However, the impact of collinearity on prediction models varies due to  
523 differences in principles. Previously, several approaches have been introduced to address  
524 collinearity problems, such as pre-selection based on thresholds, clustering predictors, and  
525 regularization techniques. Regularization is a method used to reduce the complexity of the  
526 SVM model and prevent overfitting<sup>14</sup>. Similarly, boosting-based models like AdaBoost,  
527 XGBoost, and LightGBM can effectively handle multicollinearity problems by adjusting the  
528 number of variables sampled at each split<sup>23</sup>, which acts as a regularization parameter. In  
529 contrast, MLP's ability to withstand collinearity is relatively weak, which may explain its  
530 relatively low accuracy.

531

532 The way in which heat is distributed varies greatly depending on the size of the DH network,  
533 and the proposed framework is appropriate for smaller networks where the behavior of  
534 customers has an impact on the load pattern. It is possible to apply the framework to other

535 small-scale DH networks, in order to anticipate the hourly heat demand, as long as records of  
536 the hourly heat demand and environmental factors such as wind speed, humidity and  
537 temperature are available.

538

### 539 **Interpretability**

540 Model interpretability for AI models refers to the ability to transform the training and testing  
541 processes into logical rules. The model's ability to display the significance and ranking of input  
542 variables<sup>37</sup> allows it to exhibit interpretability. The interpretability of a predictive model is  
543 crucial in evaluating the rationality of heat demands in a DH network. A lack of conformity to  
544 accepted principles in variable importance can indicate model instability or system  
545 malfunction<sup>4</sup>. Boosting-based methods are highly interpretable as they do not require the  
546 interpretation of tree structures by ML professionals, and each decision corresponds to a  
547 logical rule<sup>14</sup>. These models can output visual results of variable importance, with the weight  
548 and rank of variables differing depending on the model's inherent principles, as displayed in  
549 Figure 7. However, temperature and month were consistently the most influential variables,  
550 with humidity and holiday having a negligible impact, indicating the limited influence of these  
551 variables on heat usage.

552

553 On the other hand, SVR and MLP were less interpretable, with MLP being considered a black  
554 box method due to its difficulty in identifying the features extracted from each layer of the  
555 network. The use of a linear kernel function in SVR leads to a more interpretable model, but  
556 models with other kernels can be challenging to interpret<sup>37</sup>.

557

### 558 **Conclusion**

559 Hourly heat demand forecasting is essential for heating providers to optimize heat production  
560 and heat supply operations. This research presents an hourly heat usage prediction system  
561 that is based on standard regression algorithms, and it systematically investigates the input  
562 features' influence on the models' outcomes.

563

564 First, additional weather information, which includes the outdoor temperature, wind flow  
565 speed, and humidity of the corresponding hourly historical heat demand, were extracted  
566 during the data collection process, and they were used as the input features. After that,  
567 various data preprocessing procedures were implemented in order to clean the dataset. The  
568 preprocessed dataset was utilized in order to thoroughly analyze the common heat demand  
569 patterns. Finally, the dataset was inputted into five well-known regression algorithms, namely  
570 SVR, MLP, XGBoost, AdaBoost, and LightGBM, in order to determine what model is the most  
571 suitable for the heat usage prediction task based on standard evaluation metrics.

572

573 The XGBoost model achieved the lowest MSE via various experiments, which was less than  
574 0.01, and it was robust when the number of samples in the training dataset increased. Finally,  
575 various XAI methods, such as SHAP and PDP were applied in order to thoroughly analyze how  
576 the model gave a particular prediction. The results showed that temperature and time-related  
577 variables are the most critical features that contribute to the model's predictions.

578

579 More attention will be directed in the future toward novel heat load prediction techniques,  
580 such as multi-step ahead prediction. In addition, collecting a larger dataset with additional  
581 variables can improve the performance and efficiency of the model.

582



## 583 **Data Availability**

584 The datasets used and/or analysed during the current study available from the corresponding  
585 author on reasonable request.

586

## 587 **Code Availability**

588 The source code for all the analyses presented in this study can be found on these GitHub  
589 repositories: <https://github.com/minhdl93/HeatLoadAnalysis>

590

## 591 **Acknowledgements**

592 This work was supported by the Basic Science Research Program via the National Research  
593 Foundation of Korea (NRF) funded by the Ministry of Education (2020R1A6A1A03038540) and  
594 by a grant (20212020900150) from "Development and Demonstration of Technology for  
595 Customers Bigdata-based Energy Management in the Field of Heat Supply Chain" funded by  
596 Ministry of Trade, Industry and Energy of Korean government and by the Institute of  
597 Information and Communications Technology Planning and Evaluation (IITP) grant funded by  
598 the Korea government (MSIT) (No.2022-0-00106, Development of explainable AI-based  
599 diagnosis and analysis frame work using energy demand big data in multiple domains).

600

## 601 **Author contributions**

602 H.M. and H.S. acquired the funding and supervised the study. Y.L., L.T., and T.N. performed  
603 the data collection, preprocessing, and experimental validation. L.D. wrote the original draft.  
604 J.S. revised the manuscript. All authors have read and agreed to publish the version of the  
605 manuscript.

606

## 607 **Competing interests**

608 The authors declare that there are no conflicts of interest to report in regards to this study.

609

610

## 611 **References**

- 612 1. Lund, H.; Østergaard, P.A.; Chang, M.; Werner, S.; Svendsen, S.; Sorknæs, P.; Thorsen,  
613 J.E.; Hvelplund, F.; Mortensen, B.O.G.; Mathiesen, B.V. The status of 4th generation  
614 district heating: Research and results. *Energy* **2018**, *164*, 147-159.
- 615 2. Barone, G.; Buonomano, A.; Forzano, C.; Palombo, A. A novel dynamic simulation  
616 model for the thermo-economic analysis and optimisation of district heating systems.  
617 *Energy Conversion and Management* **2020**, *220*, 113052.
- 618 3. Dorotić, H.; Pukšec, T.; Duić, N. Multi-objective optimization of district heating and  
619 cooling systems for a one-year time horizon. *Energy* **2019**, *169*, 319-328.
- 620 4. Guelpa, E.; Verda, V. Thermal energy storage in district heating and cooling systems:  
621 A review. *Applied Energy* **2019**, *252*, 113474.
- 622 5. Buffa, S.; Cozzini, M.; D'antoni, M.; Baratieri, M.; Fedrizzi, R. 5th generation district  
623 heating and cooling systems: A review of existing cases in Europe. *Renewable and*  
624 *Sustainable Energy Reviews* **2019**, *104*, 504-522.
- 625 6. Dang, L.M.; Lee, S.; Li, Y.; Oh, C.; Nguyen, T.N.; Song, H.-K.; Moon, H. Daily and seasonal  
626 heat usage patterns analysis in heat networks. *Scientific Reports* **2022**, *12*, 1-12.
- 627 7. Xue, P.; Jiang, Y.; Zhou, Z.; Chen, X.; Fang, X.; Liu, J. Multi-step ahead forecasting of  
628 heat load in district heating systems using machine learning algorithms. *Energy* **2019**,  
629 *188*, 116085.

- 630 8. Zhao, Y.; Zhang, C.; Zhang, Y.; Wang, Z.; Li, J. A review of data mining technologies in  
631 building energy systems: Load prediction, pattern identification, fault detection and  
632 diagnosis. *Energy and Built Environment* **2020**, *1*, 149-164.
- 633 9. Guo, Y.; Wang, J.; Chen, H.; Li, G.; Liu, J.; Xu, C.; Huang, R.; Huang, Y. Machine learning-  
634 based thermal response time ahead energy demand prediction for building heating  
635 systems. *Applied energy* **2018**, *221*, 16-27.
- 636 10. Wang, Z.; Hong, T.; Piette, M.A. Building thermal load prediction through shallow  
637 machine learning and deep learning. *Applied Energy* **2020**, *263*, 114683.
- 638 11. Nageler, P.; Koch, A.; Mauthner, F.; Leusbrock, I.; Mach, T.; Hochenauer, C.; Heimrath,  
639 R. Comparison of dynamic urban building energy models (UBEM): Sigmoid energy  
640 signature and physical modelling approach. *Energy and buildings* **2018**, *179*, 333-343.
- 641 12. Westermann, P.; Deb, C.; Schlueter, A.; Evins, R. Unsupervised learning of energy  
642 signatures to identify the heating system and building type using smart meter data.  
643 *Applied Energy* **2020**, *264*, 114715.
- 644 13. Luo, X.; Oyedele, L.O.; Ajayi, A.O.; Akinade, O.O.; Owolabi, H.A.; Ahmed, A. Feature  
645 extraction and genetic algorithm enhanced adaptive deep neural network for energy  
646 consumption prediction in buildings. *Renewable and Sustainable Energy Reviews* **2020**,  
647 *131*, 109980.
- 648 14. Ntakolia, C.; Anagnostis, A.; Moustakidis, S.; Karcianas, N. Machine learning applied  
649 on the district heating and cooling sector: A review. *Energy Systems* **2022**, *13*, 1-30.
- 650 15. Guelpa, E.; Marincioni, L.; Capone, M.; Deputato, S.; Verda, V. Thermal load prediction  
651 in district heating systems. *Energy* **2019**, *176*, 693-703.
- 652 16. Rouleau, J.; Gosselin, L. Impacts of the COVID-19 lockdown on energy consumption in  
653 a Canadian social housing building. *Applied Energy* **2021**, *287*, 116565.
- 654 17. Sukparungsee, S.; Areepong, Y.; Taboran, R. Exponentially weighted moving average—  
655 Moving average charts for monitoring the process mean. *Plos one* **2020**, *15*, e0228208.
- 656 18. Harrell, F.E. General aspects of fitting regression models. In *Regression modeling*  
657 *strategies*; Springer: 2015; pp. 13-44.
- 658 19. Munkhdalai, L.; Munkhdalai, T.; Park, K.H.; Lee, H.G.; Li, M.; Ryu, K.H. Mixture of  
659 activation functions with extended min-max normalization for forex market prediction.  
660 *IEEE Access* **2019**, *7*, 183680-183691.
- 661 20. Okada, S.; Ohzeki, M.; Taguchi, S. Efficient partition of integer optimization problems  
662 with one-hot encoding. *Scientific reports* **2019**, *9*, 1-12.
- 663 21. Zhang, F.; O'Donnell, L.J. Support vector regression. In *Machine Learning*; Elsevier:  
664 2020; pp. 123-140.
- 665 22. Liu, Y.; Liu, S.; Wang, Y.; Lombardi, F.; Han, J. A stochastic computational multi-layer  
666 perceptron with backward propagation. *IEEE Transactions on Computers* **2018**, *67*,  
667 1273-1286.
- 668 23. Azmi, S.S.; Baliga, S. An Overview of Boosting Decision Tree Algorithms utilizing  
669 AdaBoost and XGBoost Boosting strategies. *Int. Res. J. Eng. Technol.* **2020**, *7*.
- 670 24. Bentéjac, C.; Csörgő, A.; Martínez-Muñoz, G. A comparative analysis of gradient  
671 boosting algorithms. *Artificial Intelligence Review* **2021**, *54*, 1937-1967.
- 672 25. Chicco, D.; Warrens, M.J.; Jurman, G. The coefficient of determination R-squared is  
673 more informative than SMAPE, MAE, MAPE, MSE and RMSE in regression analysis  
674 evaluation. *PEERJ. COMPUTER SCIENCE.* **2021**, *7*, e623.
- 675 26. Sundararajan, M.; Najmi, A. The many Shapley values for model explanation. In  
676 Proceedings of the International conference on machine learning, 2020, 9269-9278.
- 677 27. Moosbauer, J.; Herbringer, J.; Casalicchio, G.; Lindauer, M.; Bischl, B. Explaining  
678 Hyperparameter Optimization via Partial Dependence Plots. *Advances in Neural*  
679 *Information Processing Systems* **2021**, *34*, 2280-2291.
- 680 28. Pedregosa, F., Varoquaux, G., Gramfort, A., Michel, V., Thirion, B., Grisel, O.,  
681 Blondel, M., Prettenhofer, P., Weiss, R., Dubourg, V. and Vanderplas, J. Scikit-learn:

- 682 Machine learning in Python. *Journal of machine Learning research* **2011**, *12*, 2825-  
683 2830.
- 684 29. Idowu, S., Saguna, S., Åhlund, C. and Schelén, O. Applied machine learning:  
685 Forecasting heat load in district heating system. *Energy and Buildings* **2016**, *133*,  
686 478-488.
- 687 30. Bourdeau, M., qiang Zhai, X., Nefzaoui, E., Guo, X. and Chatellier, P. Modeling and  
688 forecasting building energy consumption: A review of data-driven techniques.  
689 *Sustainable Cities and Society* **2019**, *48*, 101533.
- 690 31. Saloux, E. and Candanedo, J.A. Forecasting district heating demand using machine  
691 learning algorithms. *Energy Procedia* **2018**, *149*, 59-68.
- 692 32. López, M., Sans, C., Valero, S. and Senabre, C. Classification of special days in short-  
693 term load forecasting: the Spanish case study. *Energies* **2019**, *12(7)*, p.1253.
- 694 33. Noussan, M., Jarre, M. and Poggio, A. Real operation data analysis on district  
695 heating load patterns. *Energy* **2017**, *129*, 70-78.
- 696 34. Huang, Y., Yuan, Y., Chen, H., Wang, J., Guo, Y. and Ahmad, T. A novel energy  
697 demand prediction strategy for residential buildings based on ensemble learning.  
698 *Energy Procedia* **2019**, *158*, 3411-3416.
- 699 35. Bünning, F., Heer, P., Smith, R.S. and Lygeros, J. Improved day ahead heating  
700 demand forecasting by online correction methods. *Energy and Buildings* **2020**, *211*,  
701 109821.
- 702 36. Ivanko, D., Sørensen, Å.L. and Nord, N. Selecting the model and influencing  
703 variables for DHW heat use prediction in hotels in Norway. *Energy and Buildings*  
704 **2020**, *228*, 110441.
- 705 37. Minh, D., Wang, H.X., Li, Y.F. and Nguyen, T.N. Explainable artificial intelligence: a  
706 comprehensive review. *Artificial Intelligence Review* **2022**, 1-66.
- 707 38. Greenwell, B.M. pdp: an R Package for constructing partial dependence plots. *R J.*  
708 **2017**, *9(1)*, 421.
- 709 39. Visani, G., Bagli, E., Chesani, F., Poluzzi, A. and Capuzzo, D. Statistical stability  
710 indices for LIME: Obtaining reliable explanations for machine learning models.  
711 *Journal of the Operational Research Society* **2022**, *73(1)*, 91-101.